Melting Pressure of Solid ^{3}He through the Magnetic-Ordering Transitions

J. S. Xia, W. Ni, and E. D. Adams

Department of Physics and Center for Ultra-Low Temperature Research, University of Florida, Gainesville, Florida 32611

(Received 7 December 1992)

Magnetic ordering in solid ^{3}He has been studied by measuring the melting pressure through the various phase transitions. We find a discontinuity in entropy at the high-field–paramagnetic phase transition at low fields, indicating that it is first order. The entropy discontinuity decreases as the field increases and the transition broadens, becoming second order above a field of about 0.65 T. The first precise determination of the first-order phase boundaries has been made, from which thermodynamic data not previously available are obtained.

PACS numbers: 67.80.Gb, 64.70.Kb, 65.50.+m, 67.80.Jd

Solid ^{3}He undergoes nuclear magnetic ordering near $T=1$ mK (at melting pressure in zero magnetic field) as a result of multiple exchange interactions [1,2]. The ordered phase at low fields (LFP) is antiferromagnetic with an up-up-down-down configuration of spins [3]. Above a critical field $B_{c1}=0.45$ T (for $T=0$ and melting pressure) a transition to a high-field phase (HFP) occurs [2–6]. In the HFP, lack of a frequency shift in the NMR spectrum indicates cubic symmetry [3,6]. A high magnetization is observed [4–6] and the structure is thought to be a canted normal antiferromagnet [7]. The phase diagram (to be discussed later) displaying the ordered phases, LFP and HFP, and the disordered paramagnetic phase, PP, is shown in Fig. 1.

The transitions from the PP and HFP to the LFP are known to be first order. However, there is conflicting evidence on the order of the HFP-PP transition. Some investigators have identified it as first order, at least for fields near the triple point $B_t=0.392$ T [5,8,9], while others have reported it to be second order [2,10,11]. The most successful theoretical model using two-, three-, and four-spin exchange predicts that this transition is second order [7]. Also, within the HFP a first-order transition ending in a critical point is predicted. No evidence of two transitions has been observed and it is generally believed that there is a single transition line between the HFP and PP. A recent calculation has yielded a single transition, first order at low fields, becoming second order above a tricritical point $B_{c3}=11$ T [12].

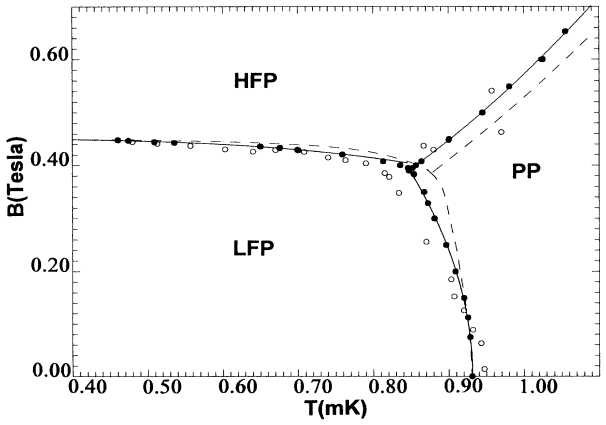

FIG. 1. Magnetic phase diagram of solid ^{3}He at melting pressure. Closed circles and solid lines, this work; open circles, Osheroff, Ref. [5]; dashed lines, Greywall and Busch, Ref. [10].

We have studied the melting pressure as function of temperature in various magnetic fields $P_m(T,B)$, from which we obtain new information on the order of HFP-PP transition and a precise phase diagram. We find the transition to be first order near the triple point with an entropy discontinuity of $\Delta S/R\ln 2=0.13$, where R is the gas constant. The entropy change at the transition decreases with increasing field, with $\Delta S\rightarrow 0$ and the transition becoming second order at about 0.65 T. These results resolve the previous discrepancies about the order of this transition and provide additional insight into the ordered phases.

The experimental arrangement, which has been described in a preliminary report [13], is similar to that of Adams, Tang, and Uhlig (ATU) [11], but with a number of significant changes. A small compact magnet inside the vacuum space supplied the magnetic field. Results for $B=0.653$ T were obtained in a cell in which the heat exchanger was located outside the field to reduce the Kapitza resistance [14]. In addition to the melting pressure cell in the field, a second one welded to the same silver platform was located in zero field. The zero-field melting pressure was used to calibrate a Pt NMR thermometer operating in the field applied to the ^{3}He and also served as an independent thermometer. The calibration temperature was $T_N(B=0)=0.931$ mK [10], which allowed the transition temperature in the field to be determined relative to the zero-field transition with a precision of 1 μK.

The entropy of the solid at melting can be obtained from dP_m/dT through the Clausius-Clapeyron equation

$$dP_m/dT=(S_l-S_s)/\Delta V\,, \tag{1}$$

where S_l and S_s are the entropies of the liquid and solid, respectively, and $\Delta V=1.314$ cm^3/mole is the volume change on melting. If the magnetic transition is first order, the melting pressure has a discontinuity in slope

dP_m/dT at the transition from which the change in entropy is found.

Data were taken with the cells warming by the heat leak at a rate of 1 to 2 μK/h, and in some cases with the cells cooling at a similar rate using computer control of the demagnetization stage. Pressures of both cells were recorded on a chart recorder as well as digitally every 5 to 15 min along with the Pt NMR temperature. Typically, three or four days were spent traversing a range of ~ 100 μK in the vicinity of the HFP-PP transition at each field. The continuous warming or cooling method allows the use of small temperature intervals ~ 2 μK in taking numerical derivatives of $P_m(T)$ to obtain the entropy. With the precision of the Pt NMR thermometer of $\sim 0.2\%$, $\Delta T \sim 50$ μK would have been required to give the same precision in dP_m/dT, if the continuous warming method had not been used.

Extensive measurements of $P_m(T,B)$ have been made in several fields between 0.405 and 0.653 T, some of which are shown in Fig. 2. Curve 1 shows both warming (1w) and cooling (1c) data for $B = 0.405$ T. (The plotted temperature is that of the thermometer attached to the cell, which differs slightly from that of the ^{3}He.) The cooling curve has been displaced by 8 μK to higher temperatures to compensate for a temperature difference of about 4 μK between the thermometer and the ^{3}He. At this field, both the LFP-HFP and the HFP-PP transitions are seen. During these transitions the system was driven further from equilibrium because of the latent heat involved, producing a plateau in the pressure versus time. This is seen clearly in the LFP-HEP transition, and although the "plateau" is less pronounced at the HFP-PP transition, this transition is also first order. The slight plateau begins at the same pressure on warming and cooling (shown by the arrow) and continues after the transition, indicating a latent heat. The discontinuous slope at the HFP-PP transition can be seen clearly from the cooling curve above the transition and the warming curve below the transition (see inset).

Because of the latent heat at the first-order transition, derivatives of $P_m(t)$ show an artificial behavior, which must be ignored, for an interval of several hours during and after the transition. Therefore, to obtain the entropy of the solid, we use the warming data below the transition and the cooling data above the transition, where both have been taken. Entropy versus temperature through the HFP-PP transition for 0.405 T (from curve 1, Fig. 2) is shown in Fig. 3, where we find $\Delta S/R \ln 2 = 0.13$.

For a field of 0.550 T, curve 2 of Fig. 2, there is a more gradual change of slope over a wider range of temperature. However, there is still a discontinuous slope at the transition, indicating a small latent heat. For 0.653 T, curve 3 of Fig. 2, the entropy changes continuously (see Fig. 3), indicating that the transition is second order at this field.

Greywall and Busch [10] have measured the heat capacity of the solid at a molar volume of 23.90 cm^3/mole (in a packed silver powder) in a field of 0.60 T. They found the transition to be second order, but somewhat broader than our results indicate. Very small density gradients of the solid confined in the powder would contribute to the broadening and might cause the transition to appear second order at this field. However, the tricritical point for 23.9 cm^3/mole is likely to be less than 0.60 T if it has

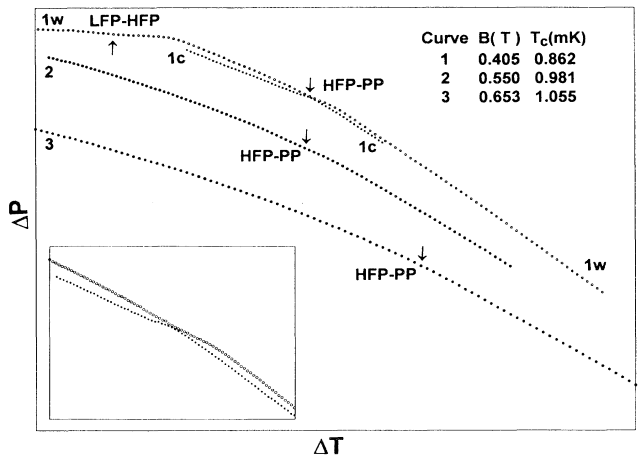

FIG. 2. Melting pressure vs temperature in the vicinity of the magnetic phase transitions for various magnetic fields. The range of ΔP is 320 Pa and ΔT is 120 μK. The inset shows details near the HFP-PP transition for 0.405 T (where $\Delta P = 60$ Pa and $\Delta T = 25$ μK). The HFP-PP transition temperatures T_c are shown in the figure.

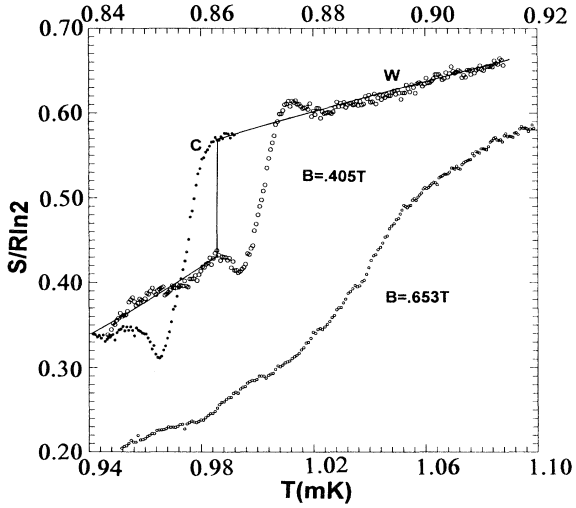

FIG. 3. Entropy vs temperature through the HFP-PP transition for various magnetic fields. For 0.405 T (upper temperature scale), the open circles are for warming (w) and the closed ones for cooling (c). In each case, the behavior for an interval of $\Delta T \sim 20$ μK following the transition is artificial. The solid lines are used to determine ΔS at the transition. For 0.653 T (lower temperature scale), the transition is second order.

a volume dependence similar to that of B_{c1} or T_N. The scaling of the specific heat with field which they found at 0.60 and 1.0 T would not be valid where the transition is first order at $B < 0.65$ T. This has important implications for the phase diagram and various thermodynamic properties (to be discussed below).

Our results that the HFP-PP transition is first order for $B < 0.65$ T and is second order at this field and above resolves most of the previous disagreement on this question. Most studies which identified the transition as first order [5,8,9] were for fields less than 0.65 T, while those identifying it as second order [10] were for $B \geq 0.60$ T. The results of ATU, reporting a second-order transition for $B \leq 0.495$ T, are very similar to the present ones. Apparently the rapid change of slope of $P_m(T,B)$ over a few μK which they saw should have been interpreted as indicating a discontinuous change in entropy.

Figure 4 shows the entropy change at the HFP-PP transition versus magnetic field. This extrapolates to zero for a field of 0.65 T, consistent with our results that the transition is second order at 0.653 T. The recent calculation of the HFP-PP transition line by Sun and Hetherington [12] yields a tricritical point at about 11 T, more than a factor of 10 greater than our results indicate. However, calculations of this type typically do not provide accurate predictions of numerical values for various features of the ordered phases.

Our determination of the phase boundaries for the three phases is given in Fig. 1. These points were determined by traversing a narrow range in temperature through the transition, both warming and cooling, at a given field. The transition temperature on warming and cooling differed by about 2 to 5 μK because of the lag of the ^{3}He behind the thermometer and the average of the two was used. In a few cases, we determined the LFP-HFP transition by sweeping the field. Temperatures were determined relative to $T_N(B=0)$ with a precision of better than 1 μK using the Pt NMR and the zero-field melting-pressure thermometers.

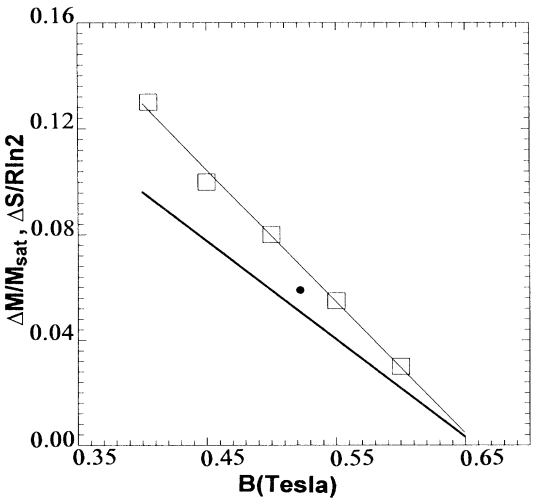

FIG. 4. Entropy (squares and light line) and magnetization (dark line) changes at the HFP-PP transition vs magnetic field. The dot is a measurement of ΔM by Osheroff, Ref. [15].

The HFP-PP transition line in Fig. 1 is given by the empirical equation

$$B = 0.304 - 0.815T + 1.08T^2 \quad (2)$$

in the region $B_t < B < 0.653$ T, where B is in tesla and T is in mK. From the slope of this curve and our measured ΔS, we can calculate ΔM, the magnetization change at the transition, from the Clausius-Clapeyron equation,

$$dT/dB = -\Delta M/\Delta S\,, \quad (3)$$

with the results shown by the bold solid line in Fig. 4 ($M_{\rm sat}$ is the saturation magnetization). Few direct measurements are available for comparison. Those of Prewitt and Goodkind [4] show a continuous change in M, probably because of density gradients. Osheroff [15] has reported one measurement at 0.522 T, which is consistent with our results.

Our LFP-PP phase boundary is represented quite well up to B_t by the equation

$$T = 0.931 - 0.545B^2\,, \quad (4)$$

with T in mK and B in tesla. If ΔM at the transition is proportional to B and there is little variation in ΔS, the B^2 dependence given in Eq. (4) would be expected [see Eq. (3)]. We obtain $\Delta M/M_{\rm sat} = 0.42B$, with B in tesla, in the low-B limit, which appears to be valid up to $B \sim 0.35$ T. The values generated by Greywall and Busch, based on $T_t = 0.880$ mK, depart from the linear dependence on B at a much lower field. Our results agree well with direct measurements at low fields [16]. Additional measurements of ΔS are needed in order to allow accurate values of ΔM to be calculated near B_t.

As shown in Fig. 1, our LFP-HFP boundary, except near T_t, can be expressed by

$$B = 0.452 - 0.092T^4\,. \quad (5)$$

This would be expected if $S \sim T^3$, characteristic of spin-wave excitations, in both phases and $\Delta M \approx$ const (since B varies little along this line). Our values for $B_{c1} = 0.452$ T (B at $T = 0$) agrees well with other determinations [5,15].

We find the triple point where the PP, LFP, and HFP meet to be at $T_t = 846$ μK and $B_t = 392$ mT. Our value for T_t is significantly lower than 880 μK inferred by Greywall and Busch [10] using various thermodynamic data and assumed scaling of the specific heat with field. The discrepancy probably results from failure of scaling near T_t. The lower value for T_t has important consequences for other quantities such as ΔM, as discussed above.

This work was supported by the National Science Foundation, Low Temperature Physics, Grant No. DMR-9019736. We acknowledge useful comments by

Professor Yasu Takano.

[1] W. P. Halperin, F. B. Rasmussen, C. N. Archie, and R. C. Richardson, J. Low Temp. Phys. **31**, 617 (1878).
[2] R. B. Kummer, R. M. Mueller, and E. D. Adams, J. Low Temp. Phys. **27**, 319 (1977).
[3] D. D. Osheroff, M. C. Cross, and D. S. Fisher, Phys. Rev. Lett. **44**, 792 (1980).
[4] T. C. Prewitt and J. M. Goodkind, Phys. Rev. Lett. **39**, 1283 (1977); **44**, 1699 (1980).
[5] D. D. Osheroff, Physica (Amsterdam) **109&110B**, 1461 (1982).
[6] E. D. Adams, E. A. Schuberth, G. E. Haas, and D. M. Bakalyar, Phys. Rev. Lett. **44**, 789 (1980).
[7] M. Roger, J. H. Hetherington, and J. M. Delrieu, Rev. Mod. Phys. **55**, 1 (1983).
[8] A. Sawada, H. Yano, M. Kato, K. Iwahashi, and Y. Masuda, Phys. Rev. Lett. **56**, 1587 (1986).
[9] T. Okamoto, H. Fukuyama, T. Fukuda, H. Ishimoto, and S. Ogawa, Physica (Amsterdam) **165&166B**, 825 (1990).
[10] D. S. Greywall and P. A. Busch, Phys. Rev. B **36**, 6853 (1987).
[11] E. D. Adams, Y. H. Tang, and K. Uhlig, J. Low Temp. Phys. **84**, 109 (1991); Y. H. Tang, E. D. Adams, and K. Uhlig, Phys. Rev. Lett. **57**, 222 (1986).
[12] Z. Sun and J. H. Hetherington, J. Low Temp. Phys. **86**, 303 (1992).
[13] J. S. Xia, W. Ni, and E. D. Adams, J. Low Temp. Phys. **89**, 355 (1992).
[14] D. D. Osheroff and R. C. Richardson, Phys. Rev. Lett. **54**, 1178 (1985).
[15] D. D. Osheroff, J. Low Temp. Phys. **87**, 297 (1992).
[16] T. Hata, S. Yamasaki, T. Kodama, and T. Shigi, J. Low Temp. Phys. **71**, 193 (1988).